

## **EXPERIMENTAL VERIFICATION OF FINITE ELEMENT MODEL TO PREDICT THE SHEAR BEHAVIOUR OF NSM FRP STRENGTHENED MASONRY WALLS**

**R.B. PETERSEN / M.J. MASIA**

PhD Candidate / Senior Lecturer  
Centre for Infrastructure Performance and Reliability  
School of Engineering  
The University of Newcastle  
Callaghan NSW Australia

**R. SERACINO**

Associate Professor  
Department of Civil, Construction, and Environmental Engineering  
North Carolina State University USA

### **SUMMARY**

A finite element (FE) model was developed to predict the behaviour of an unreinforced masonry (URM) shear wall strengthened with near surface mounted (NSM) carbon fibre reinforced polymer (FRP) strips. The FE model was verified by conducting diagonal tension/shear tests on three unreinforced and one reinforced wall with the FRP strips aligned vertically. The results of both the FE model and experimental tests were similar and showed that vertically aligned NSM FRP reinforcement was able to prevent sliding along the masonry bed joints. The load-displacement behaviour, failure modes, and the evolution of strain distributions in the NSM FRP reinforcement was determined for the specimens from the tests and the FE model and are presented herein.

### **INTRODUCTION**

Bonding FRPs to URM walls is an emerging retrofitting technique. The technique is used to increase the strength and ductility of walls subjected to in-plane and/or out-of-plane lateral loading. Two application techniques are used: externally bonding (EB) FRP sheets or plates to the wall surface; and inserting (and bonding) an FRP bar or strip into a precut groove in the surface of the masonry. The latter technique is known as near-surface mounting NSM. The NSM technique, in general, provides significant advantages over EB in that it is protected from vandalism, protected to some extent from fire and the environment, if detailed correctly may not adversely affect the aesthetics of a structure, and can generally develop a higher strain in the

FRP before debonding. For these reasons walls reinforced using NSM rectangular strips were investigated in this study.

Diagonal cracking and shear sliding along the bed joints are two failure modes of an URM wall subjected to in-plane lateral loading. In this preliminary study FRPs are used to prevent the shear sliding mode. Unlike steel, FRPs have low dowel strength, but FRPs can potentially be used to restrict crack separation in the normal direction (known as dilation) occurring during the sliding along bed joints. Dilatational behaviour upon shearing is common in frictional, cementitious materials and has been observed in masonry joints (Van der Pluijm (1998) and Van Zijl (2004)). Dilation occurring along a sliding interface (masonry bed joint) can potentially be resisted using FRP reinforcement that crosses the sliding interface perpendicularly. By resisting dilation the frictional force along the sliding interface increases, leading to a significant strength and ductility increase (noted by Van Zijl (2004) in general for structural confining members), and is related to the behaviour of the FRP-to-masonry joint where the FRP is loaded in tension, and the frictional and dilatational behaviour of the shear sliding joint. To the knowledge of the authors, this mechanism has not been previously qualified nor quantified for an FRP retrofitted masonry structure.

A FE model was built to investigate the mechanism. The FE model was validated using experimental tests on FRP strengthened URM masonry walls. The main aim of the study was to see if FRP is capable of strengthening against shear sliding by restricting the dilation movement along the sliding interface.

## EXPERIMENTAL PROGRAM

To validate the FE model a series of URM walls with and without FRP retrofitting were tested using the Diagonal Tension/Shear Test (ASTM E519-93), ASTM Standards (1993) (Figure 1a & Figure 1b). The test involves subjecting a square section of masonry, with height and length both equal to 1.2 m, to a compressive load applied along the diagonal.

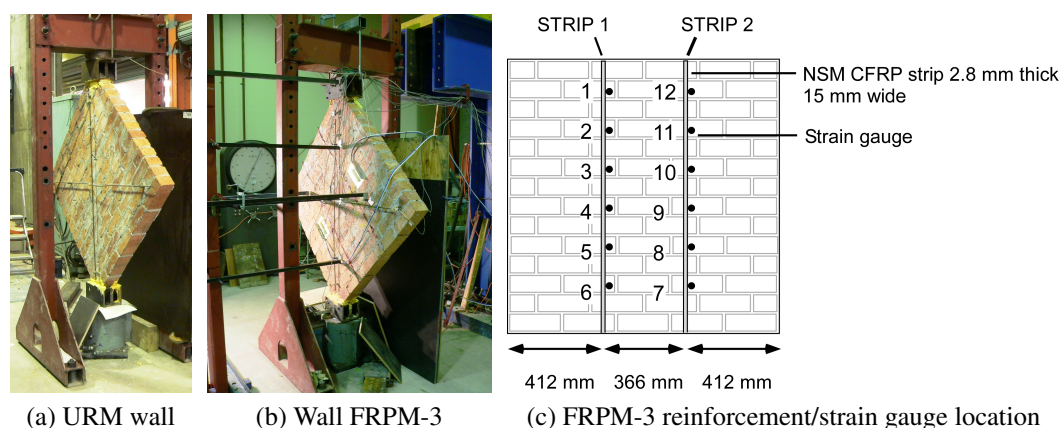


Figure 1: Diagonal Tension/Shear Test setup and reinforcement scheme

Twelve wallettes were constructed from solid clay masonry units with nominal dimensions 230 mm long, 110 mm wide and 76 mm high and mortar joints 10 mm thick. The brick unit tensile strength was determined as 4.3 MPa from lateral modulus of rupture tests (AS/NZS 4456.15), Standards Australia (2003), on a similar brick. In this paper the results of the first four wall tests

are presented. The mortar used to construct the walls was mixed in three batches, all with a mix ratio of 1:1:6 (cement:lime:sand by volume). Table 1 shows the flexural tensile bond strength results (determined by bond wrench test with 10 test replicates per batch, AS3700-2001, Standards Australia (2001)) of the masonry used to construct the walls. Note the variability between and within the mortar batches. Variability between batches was due to uncontrolled water content. Table 1 also shows the age at testing of the flexural bond strength tests and diagonal tension tests. One wall (FRPM-3) was reinforced with two carbon FRP strips 15 mm wide and 2.8 mm thick, elastic modulus equal to 210000 MPa. Carbon FRP was chosen instead of glass FRP because higher loads can be developed. The FRP reinforcement was glued, using a two-part epoxy adhesive, into rectangular grooves (approximately 20 mm deep and 6 mm wide) cut into the surface of the masonry with a circular saw and angle grinder. The FRP was flush with the surface of the wall (no brick or mortar pieces were placed over the FRP). The FRP reinforcement was used on one side of the wall and was oriented perpendicular to the mortar bed joints (Figure 1c). The reinforcement scheme was used to prevent bed joint sliding in a wall with weak bond strength. The FRP strips were constructed by gluing two FRP strips 1.4 mm thick (and 15 mm wide) together with a 'super-strength' araldite adhesive. Sandwiched between the two strips were six strain gauges placed at 170mm apart to measure the strain distribution in the FRP reinforcement during the test. A hydraulic jack was used to supply the load. Potentiometers on both sides of the wall with targets spaced at 1300 mm apart were used to measure in-plane vertical displacement as specified in ASTM E519-93, ASTM Standards (1993).

Table 1: Experimental wall data

Wall	Mortar batch	Flexural bond strength (MPa)	Age at testing (weeks)	
			Diagonal Test	Bond Wrench
URM-1-1	1	1.26 MPa (COV 32%)	8	8
URM-1-2	1	1.26 MPa (COV 32%)	8	8
URM-2	2	0.41 MPa (COV 59%)	8	8
FRPM-3	3	0.57 MPa (COV 48%)	30	14

## FINITE ELEMENT MODEL

### Masonry

To model the masonry the discrete approach, where the units and unit/mortar interfaces are modelled separately, was adopted. This model was chosen because it allows cracking and shear-induced dilation to be defined using interface elements at the unit/mortar interfaces, and it allows cracking to be defined using interface elements through the middle of a brick unit. In experimental tests cracking and sliding is generally observed at the unit/mortar interfaces and through the middle of a brick unit (Lourenço and Rots (1997)). Van Zijl (2004) provides an example of using the masonry discrete model with dilation included.

Eight-noded quadratic, rectangular plane stress elements (thickness equal to wall thickness of 110 mm) were used to model the brick units. The elastic modulus of the brick unit was experimentally determined from compression tests on masonry piers as 27600 MPa. A poisson's ratio of 0.2 was assumed (Lourenço (1996)). Six-noded quadratic, rectangular plane stress interface elements (thickness equal to 110 mm) were used to model the potential brick crack interface (at the mid-length of each brick) and the mortar joint interface. For the potential brick crack

interface elements a linear tension softening model was used. The tensile fracture energy of the brick unit was assumed as 0.025 N/mm (recommended value taken from Lourenço (1996)).

The crack-shear-crush material model, developed by Lourenço and Rots (1997) and Van Zijl (2004) and included in DIANA, de Witte (2005), was used to describe the behaviour of the mortar joint interface elements. The model is based on multi-surface plasticity and incorporates a Coulomb friction model, tension cut-off model and an elliptical compression cap model. The model also incorporates dilation behaviour that is dependent on confining pressure and shear slipping along the joints. Due to significant variability of bond strength between batches 1, 2 & 3 (see Table 1) properties for the mortar joint interface elements were estimated for the three separate mortar batches. Table 2 summarises the material properties used for the mortar interface elements.

Table 2: Material properties employed for mortar interface elements

Property		Units	Mortar Batch		
			1	2	3
Normal stiffness	$k_{n(m)}$	N/mm <sup>3</sup>	620	308	308
Shear stiffness	$k_{s(m)}$	N/mm <sup>3</sup>	260	128	128
Tensile strength	$f_{t(m)}$	MPa	0.84	0.27	0.4
Tensile fracture energy	$G_{f(m)}^I$	N/mm	0.012	0.012	0.012
Cohesion	$c_0$	MPa	0.78	0.35	0.45
Initial friction coefficient	$\Phi_i$	-	0.9	0.9	0.9
Residual friction coefficient	$\Phi_r$	-	0.9	0.60	0.65
Initial dilatancy coefficient	$\Psi_0$	-	0.75	0.75	0.75
Stress at which dilatancy is zero	$\sigma_u$	MPa	-1.2	-1.2	-1.2
Dilatancy degradation coefficient	$\delta$	-	2.75	2.75	2.75
Shear fracture energy	$G_{f(m)}^{II}$	N/mm	0.34	0.07	0.07
Compressive strength	$f_c$	MPa	32	22.4	22.4
Shear traction control factor	$C_s$	-	9.0	9.0	9.0
Compressive fracture energy	$G_c$	N/mm	25	23	23
Compressive plastic strain at $f_c$	$\kappa_p$	mm	0.019	0.013	0.013

The material properties given in Table 2 were estimated from a range of preliminary joint characterisation tests performed on similar mortar-brick joints including: 1) Compression tests on 7-brick high masonry piers; and 2) Torsion shear tests, Masia et al. (2007). Where experimental results were not available recommended values from Lourenço (1996) were used. Note that the parameters were not calibrated to fit the experimental results.

#### Attaching FRP reinforcement

FRP strips were modelled using 2-noded linear truss elements with an area of 42 mm<sup>2</sup>, elastic modulus of 210000 MPa and poisson's ratio of 0.3. To represent the NSM joint (shown in Figure 2a) in the FE model the FRP was attached to the brick unit using zero-thickness, 6-noded quadratic, interface elements (Figure 2b). The relationship between shear traction (bond) and shear relative displacement (slip) of the interface element, in the longitudinal/tensile direction of the reinforcement is defined using a local bond-slip law determined from experimental pull tests similar to those tested in Petersen et al. (2007) using the same materials (Figure 2c). The pull test involved subjecting an FRP strip, bonded to a masonry prism, to a direct tensile force. The plane

stress thickness of the interface element was set equal to the bonded perimeter of the FRP, which is approximately 33 mm. By modelling the FRP-to-masonry joint in this way, debonding of the FRP from the masonry was accounted for. To connect FRP truss elements across interfaces (brick-mortar and brick-brick interface elements) a zero-thickness node interface element was used (Figure 2d). In the longitudinal direction a high stiffness was given to the node interface element to make the FRP continuous across the joint. In the transverse direction (i.e. in the direction of brick-mortar/brick-brick sliding) a very low stiffness was given to the node interface element effectively removing any dowel strength in the FRP across the joint. The FE model was developed in this way so that the FRP could only strengthen against shear sliding if dilation occurred.

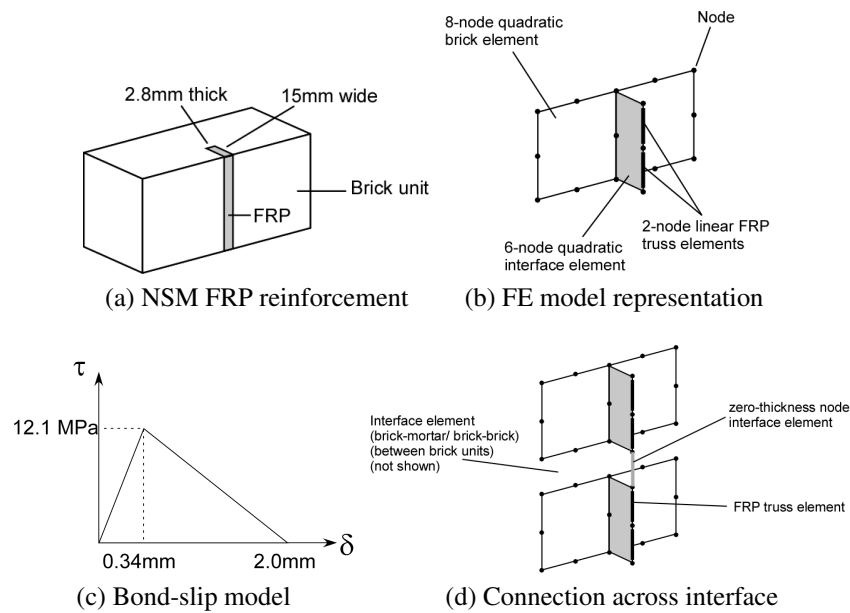


Figure 2: FRP attachment in FE model

### Model of Diagonal Tension/Shear Test

The FE models of the unreinforced walls (URM-1-1, URM-1-2 & URM-2) and reinforced wall (FRPM-3) are shown in Figure 3. As previously described rectangular quadratic plane stress elements were used for the majority of the brick units. At the support and loaded ends, however, some triangular elements were used to accommodate the boundary conditions. Nodes were fixed in both the x and y directions at the base of the model to simulate a fixed boundary condition at the bottom loading shoe. A rigid beam constraint, that keeps all nodal displacements equal, was applied to simulate the boundary condition of the top loading shoe. To model loading on the structure a displacement  $\delta$  was applied to the top corner acting downwards.

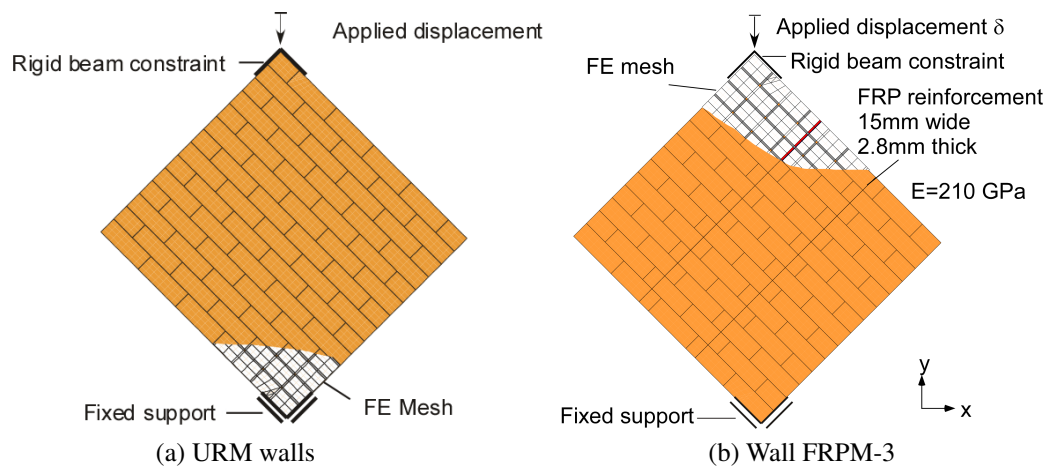


Figure 3: FE models for Diagonal Tension/Shear Test (mesh shown in cut-away)

## RESULTS OF EXPERIMENTAL AND FE ANALYSES

### Unreinforced Masonry (URM) Walls

URM-1-1 and URM-1-2 failed by diagonal cracking that occurred through both brick units and mortar joints (shown for specimen URM-1-1 in Figure 4a). As both URM-1-1 and URM-1-2 were constructed with the same mortar batch one FE model was used to simulate the behaviour. Figure 4b shows that the failure mode predicted by the FE model is similar to the experimentally observed failure mode. The load-displacement relationship of both test walls are compared with the FE model in Figure 4c. The failure loads of walls URM-1-1 and URM-1-2 were measured as 237 kN and 290 kN respectively. The FE model gives a prediction of 227 kN for the failure load which is reasonable considering the inherent variability of mortar, and the material parameters were estimated from preliminary material characterisation tests (more tests are planned to improve parameter estimation). In the experiments both walls URM-1-1 and URM-1-2 essentially behave elastically until failure, whereas the FE model shows some ductility. The source of the extra ductility may be from the assumption of a constant shear fracture energy ( $G_{f(m)}^{II}$ ) used in the model. This predicted extra ductility is not significant once reinforcement is added to the model.

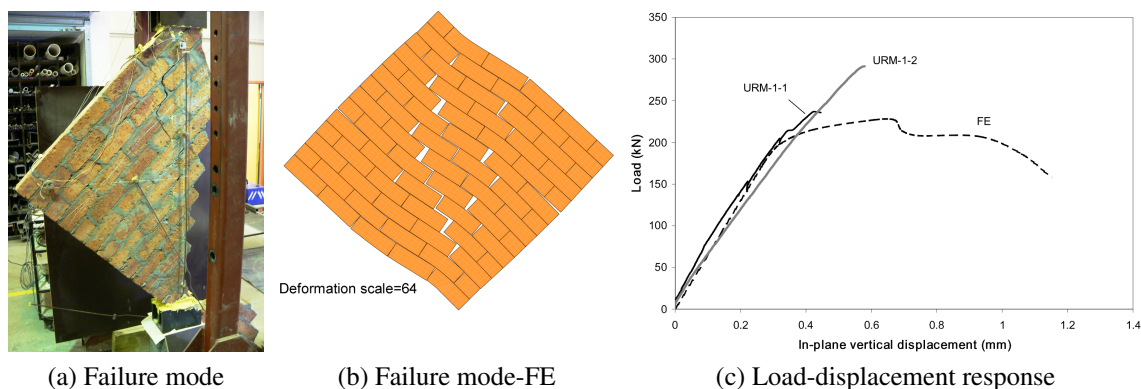


Figure 4: Results for URM-1-1 & URM-1-2

Figure 5 shows the experimental failure mode, failure mode predicted by FE model, and a

comparison between experimental and predicted in-plane load-displacement curve for specimen URM-2. In the experiment, failure occurred primarily by bed joint sliding. The FE model predicted a failure mode that was similar to that observed experimentally but considerably overestimated the ultimate strength of the wall (Curve FE in Figure 5c). A possible cause of the overprediction was the large variation of bond strength within the wall (as indicated by a coefficient of variation of the bond strength for the mortar batch used to construct the wall of 59% - refer to Table 1). Two out of ten joints tested to determine the bond strength broke during test setup meaning zero bond strength. It is possible that in the wall, joints with very little to no bond strength were present which could have led to the reduced ultimate strength. To illustrate the effect of mortar joints with low bond strength on the model, an analysis was performed with tensile strength of the mortar joint  $f_{t(m)} = 0.01$  MPa and cohesion of the mortar joint  $c_0 = 0.02$  MPa (Curve FE-Low bond strength in Figure 5c). The experimental result fits between the average and the lower bound load-displacement response of the FE model.

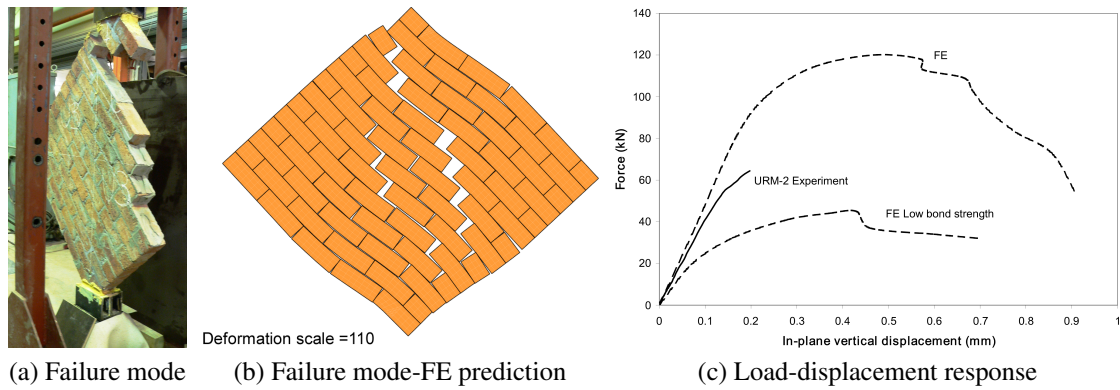


Figure 5: Results for URM-2

## FRP Retrofitted Wall

The experimental load-vertical displacement response of wall FRPM-3 up to approximately 4.5 mm is shown in Figure 6 (solid line). Plots of strain in the FRP, determined from strain gauges (refer to Fig 1c for strain gauge locations), versus in-plane vertical displacement are shown in Fig 7 for both FRP strips (solid lines).

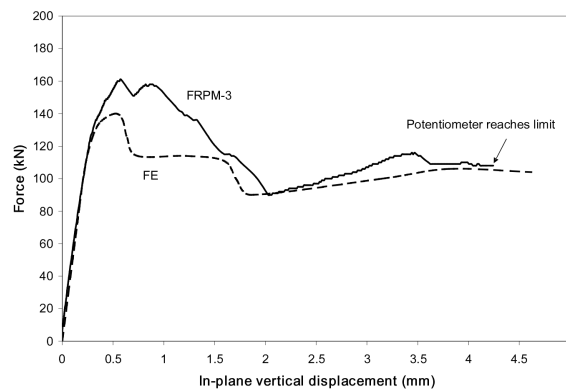


Figure 6: Load-displacement response

Before the vertical displacement reached approximately 0.25 mm the wall behaved elastically



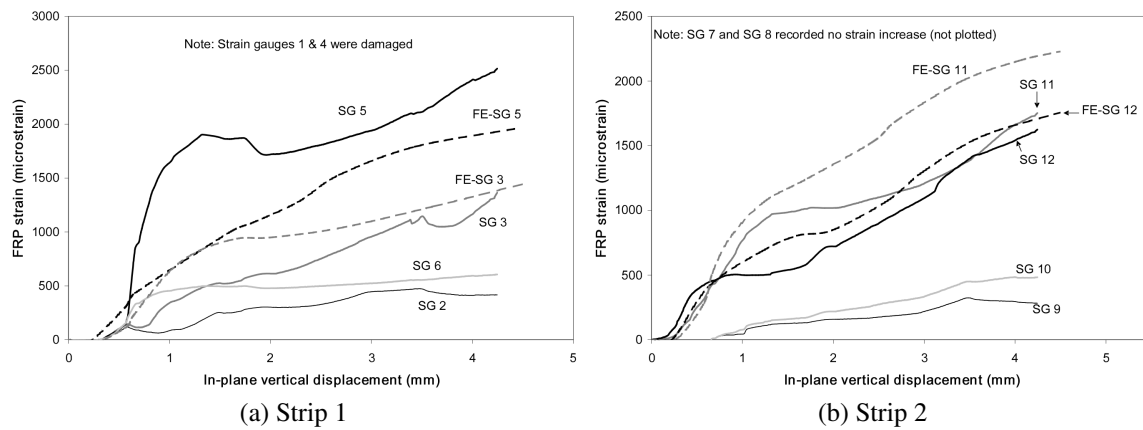


Figure 7: Strain in FRP strips vs in-plane vertical displacement

and the FRP remained inactive. After the elastic region, cracks began to form (indicated by stiffness reduction in the load-displacement curve) and the FRP began to take load (indicated by increasing strains in both FRP strips). Note that at this point the unreinforced specimens would have lost all load carrying capacity, but in the case of the reinforced specimen the FRP held the wall together and transferred a large amount of shear stress through the cracks. The reinforced specimen attained a maximum load of 160 kN. At this point a fully developed shear crack had formed (crack pattern shown in Figure 8a and Figure 8b). Note that for clarity the crack pattern at the end of testing has been shown.

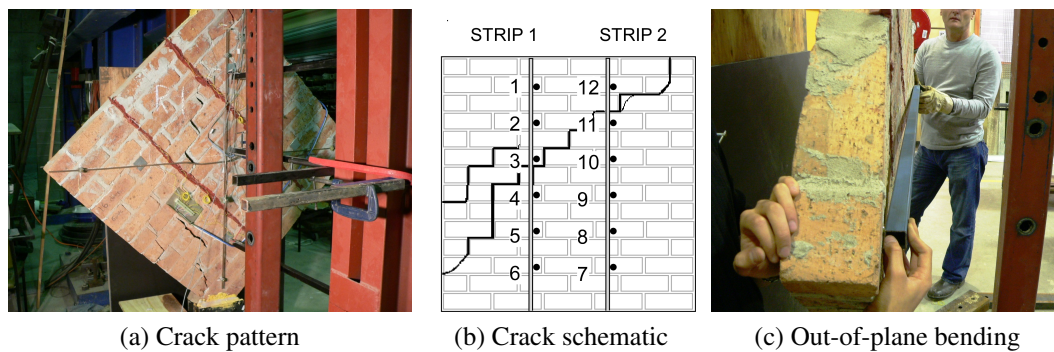


Figure 8: Test observations for FRPM-3

After ultimate load, with increasing vertical displacement, the top section of the wall gradually slid relative to the bottom section of the wall along the crack, the load-displacement response softened, the strains in the FRP strips increased and the FRP bent. After 2 mm of vertical displacement the specimen load gradually increased and a residual frictional load of 100 kN was established. The strain distribution in both strips, at a vertical displacement of 4 mm, is shown in Figure 9 (solid line). By referring Figure 9 to Figure 8b, where the strain gauge positions relative to the crack are shown, it can be seen that the maximum strains are recorded in the vicinity of the shear sliding crack. The increase in FRP strain in regions adjacent to shear sliding cracks as sliding increased indicates that the FRP strips were strained by shear induced dilation. Figure 6 does not give a complete representation of how much displacement capacity the wall had. Potentiometers used to measure the in-plane vertical displacement reached their travel capacity shortly into the test. The in-plane displacement was, however, measured at the hydraulic jack level with a larger potentiometer and this indicated that the wall was able to deform at least



25 mm. This is a large increase in ductility over the unreinforced specimens. Significant out-of-plane displacement occurred during the test because of the one-sided reinforcement scheme (shown in Figure 8c). At the later stages of the test the residual load reduced to approximately 60 kN. This reduction in load could have been due to the large out-of-plane warping that was occurring in the specimen. To avoid a potentially dangerous out-of-plane failure the test was stopped at this stage.

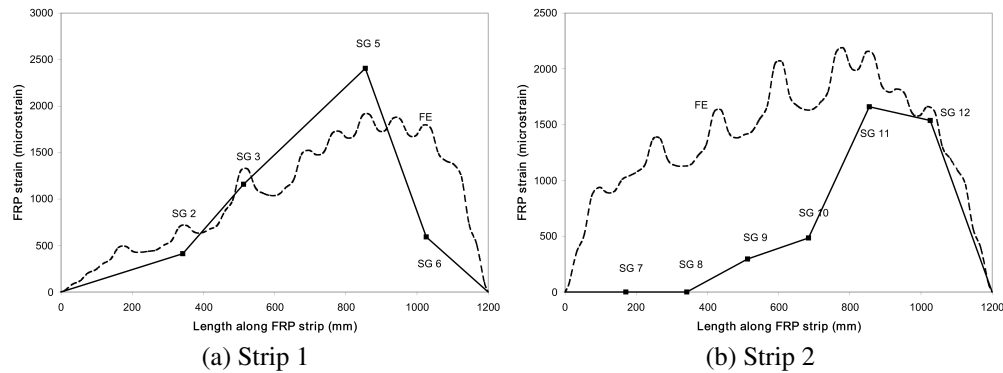


Figure 9: Strain distribution in FRP strips at 4 mm in-plane vertical displacement

Results of the FE analysis are plotted in Figure 6, Figure 7 and Figure 9 using broken lines. Figure 10 shows the crack pattern predicted by the FE model at a vertical displacement of 4 mm.

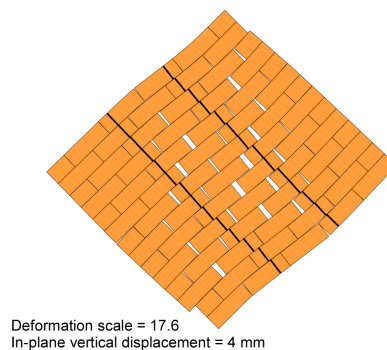


Figure 10: Results for FRPM-3

The FE model reproduced the key behaviours observed during the experiment: the FRP plates became active once masonry cracks developed at a vertical displacement of 0.25 mm; the load displacement response softened gradually as the sliding crack developed and strains in the FRP increased (at a similar rate observed in the experiment); and a residual friction plateau was established. The load displacement response predicted by the FE model follows closely the experimental response, with a predicted ultimate load of 140 kN (88% of the experimental ultimate load), and a residual load close to 100 kN. The main difference between the experimental results and the FE model was the distribution of cracking. In the FE model sliding cracks were well distributed (shown in Figure 10 and from strain distribution in the plates, Figure 9). One possible reason for the discrepancy could be due to out-of-plane deformation in the experiment not allowing redistribution of forces within the wall (and hence more crack spreading). The plane stress FE model did not include out-of-plane effects. Note that a sliding plane developed in the model, that was similar to that observed in the experiments, starting two courses from the top and ending two courses from the bottom.

## CONCLUSIONS AND FUTURE WORK

The FE model was built so that it did not include dowel strength in the FRP and therefore sliding resistance could only be increased if the FRP strips acted to resist shear induced dilation. The model presented reproduced the key behaviours of the experimental test and this indicates that the mechanism, where the FRP increases shear sliding friction by preventing dilation, is realistic. The experiment and FE analyses show that the ductility of the masonry wall was increased significantly. Future work includes testing more walls with different reinforcement schemes and performing more material characterisation tests to improve estimates for material parameters used in the model.

## ACKNOWLEDGEMENTS

The authors gratefully acknowledge the support of technical staff of the Civil, Surveying and Environmental Engineering Laboratory at The University of Newcastle. Financial support for this project was provided by the Australian Research Council under Discovery Project DP0559706.

## REFERENCES

- ASTM Standards (1993). ASTM E 519–93: Standard Test Method for Diagonal Tension (Shear) in Masonry Assemblages. American Society for Testing and Materials. Philadelphia.
- de Witte, F. C. (2005). DIANA 9 users manual. TNO DIANA. Delft, The Netherlands.
- Lourenço, P. B. (1996). A user/programmer guide for the micro-modeling of masonry structures. TU-DELFT report no. 03.21.1.31.35, Delft University of Technology.
- Lourenço, P. B. and Rots, J. G. (1997). A multi-surface interface model for the analysis of masonry structures. *Journal of Structural Engineering*, 123(7):660–668.
- Masia, M. J., Han, Y., Player, C. J., Correa, M. R. S., and Page, A. W. (2007). Torsion shear test for mortar joints in masonry: Preliminary experimental results. In *Tenth North American Masonry Conference*, St Louis, Missouri, U.S.A. 3-6 June, CD proceedings.
- Petersen, R. B., Masia, M. J., and Seracino, R. (2007). Influence of plate orientation and amount of precompression on the bond strength between NSM CFRP strips and masonry. In *Tenth North American Masonry Conference*, St Louis, Missouri, U.S.A. 3-6 June, CD proceedings.
- Standards Australia (2001). AS3700-2001 Masonry Structures: Appendix D - Method of test for flexural strength. Standards Australia, Sydney.
- Standards Australia (2003). AS/NZS 4456.15:2003: Masonry units, segmental pavers and flags-Methods of test. Method 15: Determining lateral modulus of rupture. Standards Australia, Sydney.
- Van der Pluijm, R. (1998). Overview of deformation controlled combined tensile and shear tests. Rep.tue/cco/98.20, Eindhoven Univ. of Technology, Eindhoven, The Netherlands.
- Van Zijl, G. P. A. G. (2004). Modeling masonry shear-compression: Role of dilatancy highlighted. *Journal of Engineering Mechanics*, 130(11):1289–1296.